Available online at www.CivileJournal.org

Civil Engineering Journal

(E-ISSN: 2476-3055; ISSN: 2676-6957)

Vol. 11, No. 04, April, 2025

Sustainable Asphalt Mixtures Comprising Steel Slag Filler and SBS-Modified Binder: An Experimental Investigation

Ahmed F. Al-Tameemi [1], Zahraa T. Al-Fayyadh [1], Hasan Al-Mosawe [1*], Yu Wang [2], Aous A. Moyet [3]

[1] *Department of Civil Engineering, College of Engineering, Al-Nahrain University, Baghdad 10071, Iraq.*

[2] *School of Science, Engineering and Environment, University of Salford, Manchester M5 4WT, United Kingdom.*

[3] *Department of Civil Engineering, College of Engineering, University of Baghdad, Baghdad 10071, Iraq.*

Received 07 January 2025; Revised 17 March 2025; Accepted 21 March 2025; Published 01 April 2025

Abstract

Utilizing steel slag powder as a mineral filler in asphalt concrete mixtures has garnered increasing attention due to its attractive benefits in both sustainability and material properties. The paper aims to critically evaluate the replacement of mineral filler with steel slag to produce a sustainable mixture. The replacement was made at 3 varied contents, i.e., 0%, 50%, and 100%, and meanwhile working together with a modified asphalt binder using 4% styrene-butadiene-styrene polymer. All designed mixtures were tested for volumetric properties and Marshall stability; an indirect tensile test was performed to determine the moisture susceptibility of all the mixtures of optimized binder content. At last, Scanning Electron Microscopy (SEM) and Energy Dispersive X-ray (EDX) analyses were performed to examine the crystal structure, microscopic attributes, and chemical composition of the steel slag particles and the limestone dust and compare their differences. The study showed that steel slag used for mineral filler can significantly enhance Marshall properties and moisture susceptibility of asphalt mixtures. Working together with the SBS-modified binder, the positive effect was further pronounced. SEM analysis revealed that steel slag has a rough, angular surface texture with a high porosity and specific surface area. EDX analysis confirmed the pozzolanic composition of steel slag.

Keywords: Sustainability; Industrial By-Product; Steel Slag; Asphalt Concrete; Material Properties; SBS-Modified Binder.

1. Introduction

Asphalt concrete is the most popular material in road pavement engineering. However, the construction and maintenance of asphalt pavement have high costs both economically and environmentally. To adapt to sustainable development and climate change, modifying asphalt binder to improve its properties for better performance and durability and, meanwhile, using recycled materials for the aggregate and mineral filler to reduce the cost and environmental impact have increasing interest both in practice and research [1-3].

Styrene-Butadiene-Styrene (SBS) rubber is popularly used as an asphalt modifier. Previous studies have demonstrated that concrete using SBS-modified asphalt has better crack resistance at both high and low temperatures, as well as enhancement in other pavement performance properties [4, 5]. Studying the SBS modification at 1, 2, 3, 4, and 5% by the total weight of asphalt binder, Mahmood and Kattan [6] noticed that SBS increased the binders' viscosity, elastic recovery, and softening point but decreased penetration, while the asphalt performance grade (PG) enhanced at both high and low temperatures. Their results indicated that the mixture of 3% SBS in binder showed the maximum

* Corresponding author: hasan.m.al-mosawe@nahrainuniv.edu.iq

http://dx.doi.org/10.28991/CEJ-2025-011-04-04

tensile strength and rutting resistance. Previous studies have also noticed that the stability of SBS-modified asphalt deteriorates with aging, particularly under the situation of coupled heavy traffic load and extreme temperature variation [7, 8]. Using SBS together with crumb rubber materials (CRM) to modify asphalt binder has also been investigated by many researchers. For example, Li et al. [9], through the rutting test, asphalt bond strength test, moisture-induced sensitivity test, and low-temperature cracking resistance test, found that SBS-CRM asphalt can greatly increase both the moisture resistance and low-temperature cracking resistance. Abed et al. [10] compared asphalt modification using SBS alone and a mixture of SBS and polyvinyl chloride (PVC). Comparing the effect on the hot mix asphalt concrete using fine and coarse aggregate, respectively, they found that, on the improvement by SBS, PVC can further improve the mechanical rigidity and strength, but the material toughness on energy absorption degraded.

Steel slag (SS) is a byproduct generated during the steel manufacturing process when molten steel is separated from impurities [11]. SS contains abundant minerals of significant economic value. Due to its favorable pozzolanic properties, SS has been widely used in large-scale building construction projects as a cementitious material, working in conjunction with Portland cement [12, 13]. In pavement engineering, SS has been utilized for sub-base stabilization to prevent the expansion of clayey soils [14] and as a substitute for natural aggregates [15], thereby enhancing pavement foundation strength and reducing maintenance costs [16, 17]. Additionally, SS has been directly incorporated into asphalt concrete as both coarse aggregate and micro filler in the wearing course, improving resistance to rutting, fatigue, skid, and creep [17]. Hosseinzadeh et al. [18] reported that using electric arc furnace (EAF) steel slag as fine aggregate enhanced the moisture resistance, Marshall stability, and indirect tensile strength of hot mix asphalt mixtures. Similarly, Oluwasola et al. [19] found that replacing natural granite aggregates with EAF slag and copper mine tailings (CMT) improved the performance characteristics of asphalt mixtures. Investigating its application in wearing courses, base, and sub-base layers, a recent study by Hassan et al. [20] recommended replacing 25–30% of the coarse aggregate with SS. However, modeling based on the Mechanistic-Empirical Pavement Design Guide (MEPDG) rutting model indicated that the use of SS increases rut depth. Nevertheless, life cycle cost (LCC) analysis estimated approximately a 29.4% cost saving when SS is used in both the base and sub-base layers, assuming zero material cost for SS.

SS itself exhibits high compressive strength and durability. Its physical properties, summarized in Table 1, endow it with superior mechanical characteristics, including strength, hardness, and moisture resistance. Furthermore, SS has high porosity, resulting from microscopic air bubbles formed during the rapid cooling of molten metal in the steel manufacturing process [21, 22]. The alkaline nature of SS promotes strong chemical binding or adhesion with asphalt, which is inherently acidic [22]. As shown in Table 2, the chemical composition of SS, rich in calcium and magnesium oxides, facilitates stronger bonding with asphalt resin compared to conventional minerals like limestone [23, 24]. This improved bonding enhances the performance of asphalt concrete mixtures in terms of moisture resistance, stiffness, fatigue life, and rutting resistance [17, 25–28].

Moreover, the crystalline structure of SS improves particle interactions with principal elements such as calcium, silicon, and iron, significantly boosting asphalt mixture performance in key areas [29]. It is also important to note that stockpiling SS poses environmental concerns due to the potential leaching of heavy metals [30]. Incorporating SS into asphalt concrete matrices mitigates this risk by preventing direct exposure to rainfall, thereby substantially reducing leaching and minimizing its environmental impact.

Table 1. Typical physical properties of steel slags [31]

Physical properties	Unit	Values
Impact value	%	17
Compressive strength	N/mm^2	200
Particle density	g/cm^3	3.6
Water absorption	%	1
Polishing resistance	PSV	57
Freeze/thaw resistance	%	Less than 0.5

Table 2. Typical chemical composition of steel slags [31]

Constituent	Percent by weight%
CaO	35-45
SiO_2	11-17
Al_2O_3	1-6
MgO	2-9
FeO	16-26
MnO	2-6
P_2O_5	1-2
S	Less than 0.2
Cr_2O_3	0.5-2

The combined benefits of binder modification and the use of recycled waste materials have garnered significant interest. Zeinoddin et al. [32] utilized steel slag (SS) and an amino-based resin-modified asphalt, which helped reduce the binder's viscosity to facilitate the production of warm mix asphalt. Experimental results demonstrated acceptable moisture resistance and an improvement in rutting resistance compared to mixtures using a neat asphalt binder. Abbas [33] investigated the use of Styrene-Butadiene Rubber (SBR) in combination with fly ash. Marshall property tests revealed that increasing the content ratio of fly ash and SBR resulted in higher sample stiffness. More recently, Abbas and Abed [34] studied the use of a Styrene-Butadiene-Styrene (SBS) modified asphalt binder along with partial replacement of limestone filler with cement kiln dust (CKD). Their findings indicated that the addition of SBS increased the binder’s hardness, while 25% and 50% replacement of filler with CKD enhanced the stability, plastic flow, and indirect tensile strength of the asphalt concrete samples.

Nie et al. [35] investigated the modification effects and mechanisms of using recycled glass fiber (GF) from wind turbine blades (WTB) in SBS-modified asphalt. A GF-WTB/SBS composite-modified asphalt was developed, and its performance was assessed using a dynamic shear rheometer (DSR) and a bending beam rheometer (BBR). The results demonstrated that a moderate addition of GF-WTB improved both the high-temperature performance and low-temperature crack resistance of the asphalt, due to the compatibility between SBS and GF-WTB, which enhanced the asphalt's elasticity and toughness. A recent study by Li et al. [9] explored the use of steel slag (SS) as a coarse aggregate in asphalt concrete combined with an SBS/crumb rubber (CR) composite-modified asphalt binder. Their findings showed that under both high and low temperature conditions, SS and SBS/CR composites exhibited improved adhesion due to enhanced electrostatic interactions. Additionally, Shen et al. [36], through SEM and FTIR analysis of aggregate morphology and the microstructure of the asphalt binder–aggregate matrix, revealed that SS provides much stronger adhesive bonding with rubberized asphalt binder compared to conventional aggregates.

While the physical characteristics and chemical composition of SS are comparable to those of conventional limestone dust used as mineral filler in asphalt concrete, limited research has been conducted on the combined use of SBS-modified asphalt binder with SS as a mineral filler substitute. Against this backdrop, a comprehensive experimental study was conducted, as reported in this paper, to evaluate the performance of asphalt concrete mixtures incorporating SS at zero, half, and full replacement levels of conventional limestone dust as the mineral filler, alongside the use of both neat and SBS-modified asphalt binders. The results demonstrated the beneficial effects of the combined use of SBS and SS on the Marshall properties and moisture susceptibility of asphalt concrete mixtures. Finally, SEM and EDX examinations were performed to gain deeper insight into the microscopic characteristics and chemical composition of the filler materials, providing analytical explanations for the observed improvements in material properties and performance.

2. Experiments

The experimental methodology of the current study was conducted in three phases. The first phase involved the preparation of raw materials following the research plan, including aggregate, mineral fillers (traditional limestone dust and steel slag powder), and asphalt cement (both neat and SBS-modified). The second phase focused on mix design, experimental setup, and test material properties and performance on durability. In the third phase, the microstructural characteristics and composition of the fillers were analyzed using SEM and EDX technology. The overall experimental framework is illustrated in Figure 1.

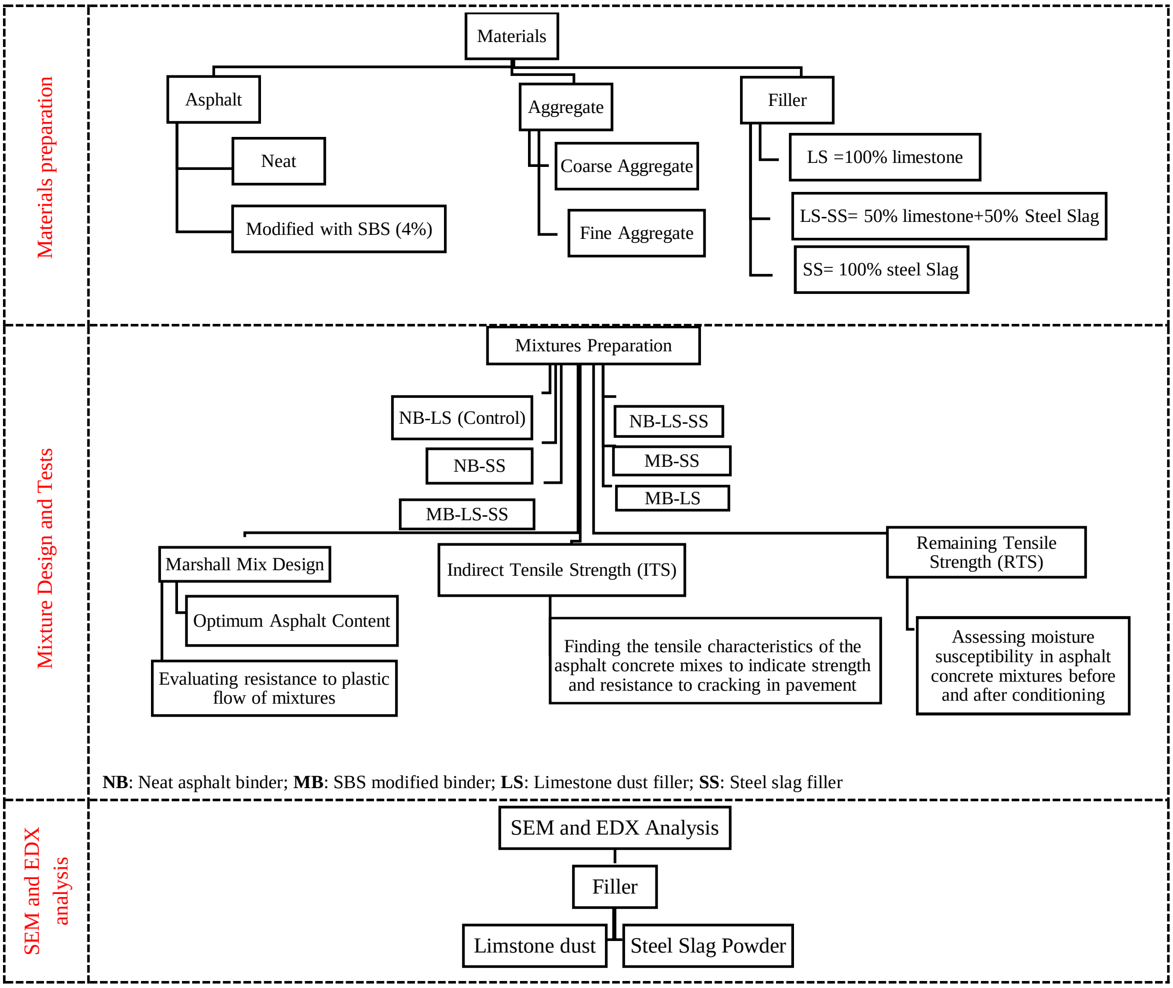

Figure 1. The flow chart of experimental study

2.1. Raw Materials

2.1.1. Asphalt Binder

Two types of asphalt binder were used. One is a neat asphalt cement (NB), brought from Al-Daura Refinery in Baghdad, Iraq, which has penetration grades of 40–50. The physical properties of the asphalt binder were examined against the standard, State Corporation for Roads and Bridges (SCRB 2003), which are listed out in Table 3. The other one (MB) is a modification of the NB, which contains 4% styrene-butadiene styrene (SBS) rubber by total weight of binder.

Table 3. Physical properties of asphalt binder

Test	ASTM Designation	Unit	Results	SCRB Specification limits
Penetration (25°C,100g,5 sec)	D-5	1/10 mm	46	40-50
Softening point (Ring& Ball)	D-36	°C	53	---
Ductility (25°C,5cm/min)	D-113	cm	110	>100
Specific gravity at 25°C	D-70	---	1.03	---
Flash, Point (Cleveland Open up)	D-92	°C	243	>232

2.1.2. Aggregate

The aggregate was supplied by the Al-Nibaie quarry in Baghdad, Iraq. The physical attributes of the aggregate are listed in Table 4 against the SCRB (2003) specification for surface layer design. Figure 2 illustrates the aggregate particle gradation.

Table 4. Physical properties of aggregate

Property	ASTM Designation	Coarse aggregate	Fine aggregate	SCRB Specification
Bulk Specific Gravity	ASTM C127-15 [37]	2.613	2.621	-
Apparent Specific Gravity	ASTM C127-15 [37]	2.678	2.683	-
Percent Water Absorption	ASTM C127-15 [37]	0.91	0.94	-
Toughness (Los Angeles Abrasion)	ASTM C131/C131M-20 [38]	20.8%	-	Max. 35%
Soundness loss by sodium sulfate solution%	ASTM C88/C88M-18 [39]	4.1 %	-	Max 12 %

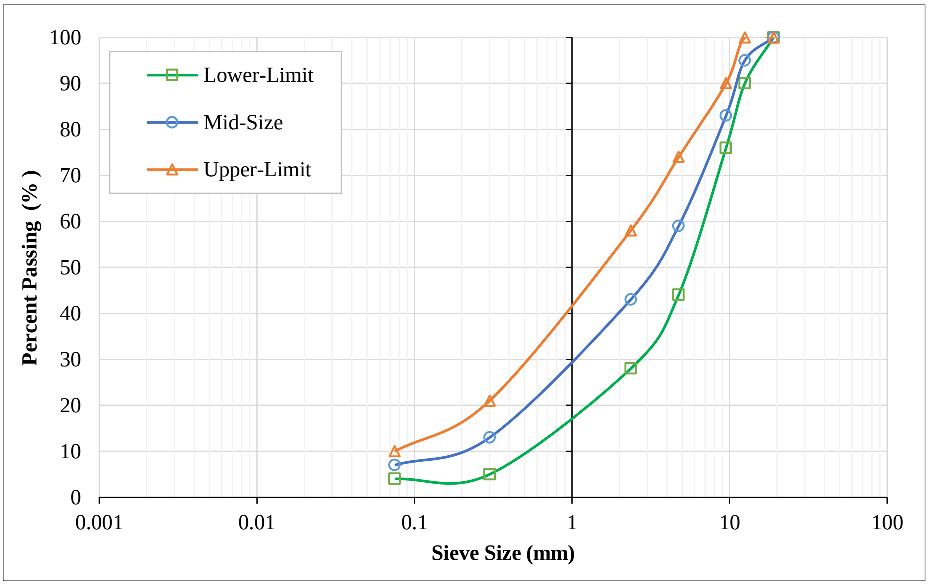

Figure 2. Aggregate particle gradation against the limits for surface course

2.1.3. Mineral Filler

Both limestone dust (LS) and steel slag (SS) powder, which were obtained from respective manufacturers' factories located in Karbala Governorate, Iraq, were utilized for the mineral fillers. The physical characteristics of the LS and the SS are listed in Table 5.

Table 5. Physical properties of mineral filler

Property	Steel Slag	Limestone
Specific gravity	3.6	2.77
Specific surface area	330 m^2/kg	309 m^2/kg
passing sieve No.200 (0.075 mm)	98	

2.2. Marshall Test

After material preparation and initial testing, the Marshall stability test was conducted to determine the optimum asphalt binder content and key volumetric properties for all the designed asphalt concrete. As listed out in Table 6, there are total six concrete designs using two different binders, i.e., the NB and MB, together with three percentages of the LS replacement by SS at 0%, 50%, and 100%. For each of the design, five sub-mixtures were made, which have varied asphalt binder contents at 4, 4.5, 5, 5.5 and 6% by total aggregate weight.

Table 6. The Designed Asphalt Concrete Mixtures for the Research

Mixtures	Asphalt binder %	SBS %	Limestone dust %	Steel slag powder %	OAC %
NB-LS (Control)	100	0	100	0	4.8
NB-LS-SS	100	0	50	50	4.9
NB-SS	100	0	0	100	5.08
MB-LS	96	4	100	0	4.75
MB-LS-SS	96	4	50	50	5
MB-SS	96	4	0	100	5

Three specimens were made for each of the sub-mixtures following the specific procedure (MS-2, Asphalt Mix Design Methods, Asphalt Institute, 2015) [40] and tested for their Marshall properties (ASTM D6926-20). The final Marshall properties of each sub-mixture took the average of the measurements of its three specimens. At last, the optimum binder content (OAC) for each mixture design, which is listed in Table 6, takes the average value of the binder contents of the sub-mixtures that had the maximum unit weight, maximum stability, and 4% air void content, respectively, in the Marshall test. After the Marshall test for OAC, the six designed mixtures in Table 6 were reprepared in terms of the determined OBC for each of them. Thereafter, the Marshall test was conducted again for each of these mixes in triplicate for their Marshall material properties. Figure 3 shows the setup of the Marshall test and the specimens for the test.

Figure 3. Marshall test equipment and the specimens in water path at 60°C (ASTM D6926-20) before test

2.3. Indirect Tensile Test (IDT)

After completing the Marshall tests, the six designed mixtures were evaluated for their durability using the Indirect Tensile (IDT) test method (ASTM D6931) to assess moisture susceptibility. Initially, the prepared mixtures were divided into two groups. For each group, cylindrical specimens were cast in triplicate for each mix. The specimens were molded using cylindrical molds with two open ends, measuring 101.6 mm in diameter and 63.5 mm in height. The mixtures placed into the molds were compacted using a Marshall compactor, applying 45 blows to each end of the cylindrical specimens to achieve an air void ratio of approximately 7.0 ± 0.5%.

Subsequently, all specimens in the first group were tested in an unconditioned state. These specimens were first placed in a 25°C water bath for one hour, then removed, towel-dried, and tested for their Indirect Tensile Strength (ITS) at room temperature using the IDT test. Meanwhile, the specimens in the second group were tested in a conditioned (moisturized) state. To prepare them, the specimens were first subjected to a vacuum of -70 kPa in a flask filled with 25°C water for five minutes to achieve saturation. They were then wrapped in plastic bags and placed in a freezer at approximately -18°C for 16 hours. After removal from the freezer, the specimens were immediately immersed in a 60°C water bath for 24 hours, followed by an additional hour in a 25°C water bath. Finally, the specimens were removed and tested for ITS at room temperature using the IDT method.

During the IDT tests, a compressive load was applied at a constant rate of 50 mm per minute until the specimens failed or split. The maximum recorded load represented the ITS value of each specimen. Figure 4 illustrates the IDT test setup and an example of a specimen after failure.

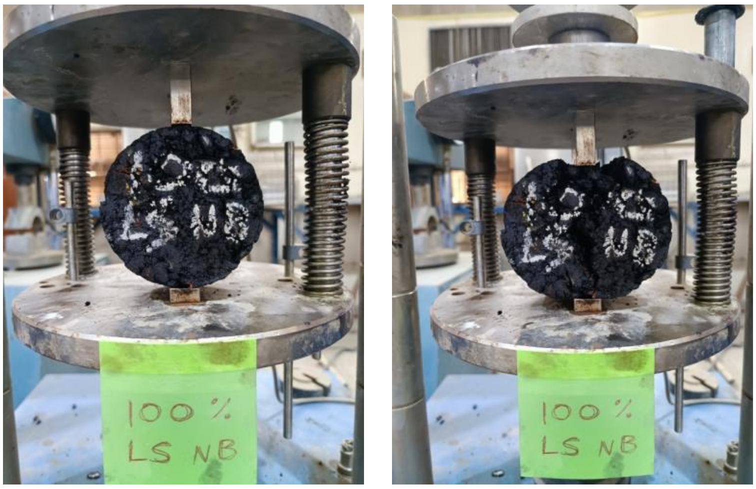

Sample under loading Sample split

Figure 4. The indirect tensile test

3. Results and Discussion

3.1. The Marshall Test

Figure 5 compares the densities of the six concrete mixtures studied in Table 6. It can be seen that both the SBS asphalt binder (MB) and SS filler make the density of mixtures increase because the SBS and the SS have a higher specific weight than the asphalt binder (NB) and the LS filler, respectively.

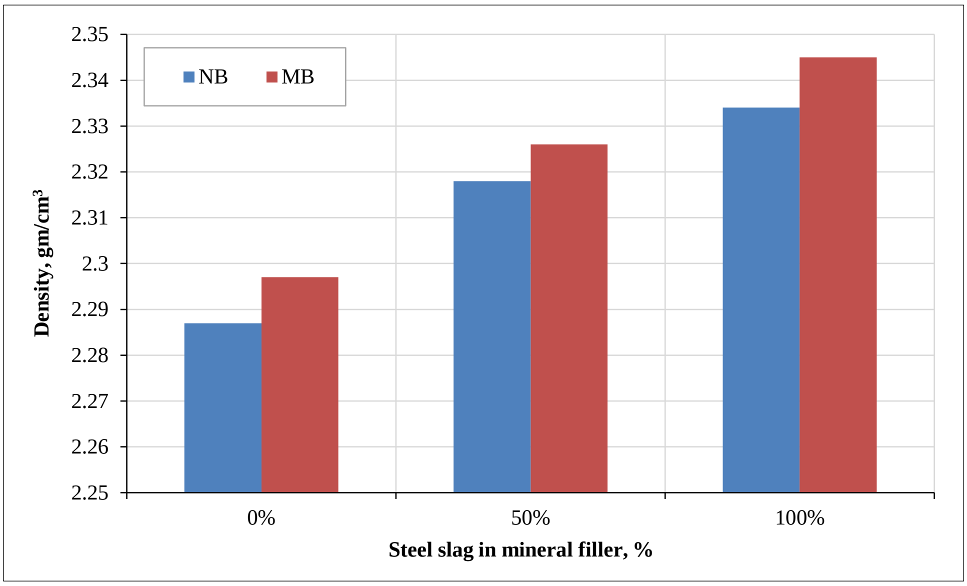

Figure 5. The density of mixtures

Figure 6 shows the Marshall stability test results of the mixtures. It can be seen that both the SBS binder modifier and the SS mineral filler respectively help enhance the Marshall stability of mixtures. A comparison shows that the mixture using the MB binder only (i.e., MB-LS) has an almost equivalent stability to that using the NB binder but 100% SS filler (i.e., NB-SS). Overall, the combined use of the MB binder and the SS filler produced progressive improvement in mixture stability, with the best benefit achieved by the mixture using 100% SS filler (MB-SS). This finding is in agreement with a previous similar study but using SS to replace copper mine tailings for mineral filler [19].

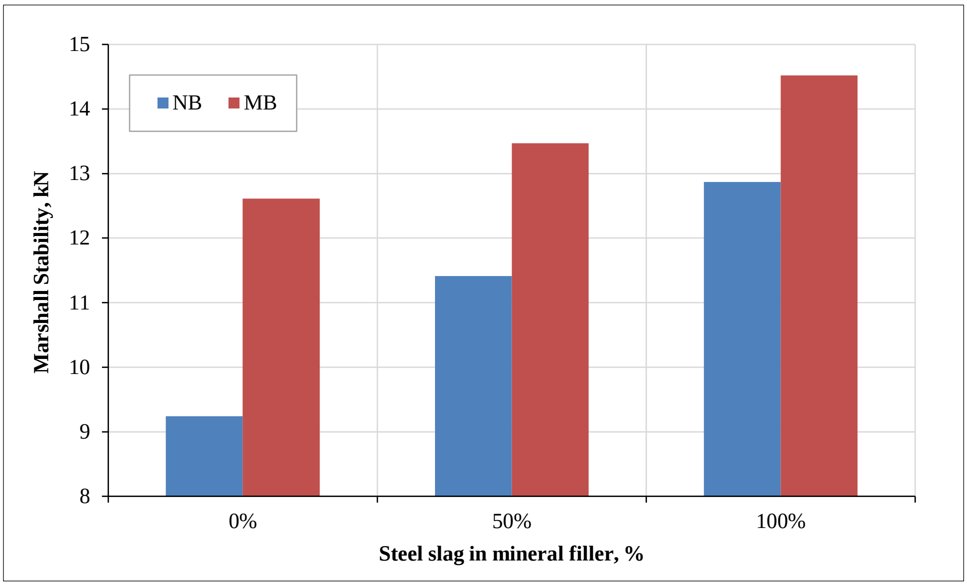

Figure 6. the Marshall stability of mixtures

Figure 7 presents the measured Marshall flow values, which show that both the MB binder and the SS filler help reduce the plastic deformation of mixtures. The results are aligned with the property of the SBS, which is stiffer than neat asphalt binder, and the characteristics of SS powder, which has a higher porosity and rough surface texture in comparison with limestone dust. These binder properties and filler characteristics working together help enhance the rigidity of the mixtures.

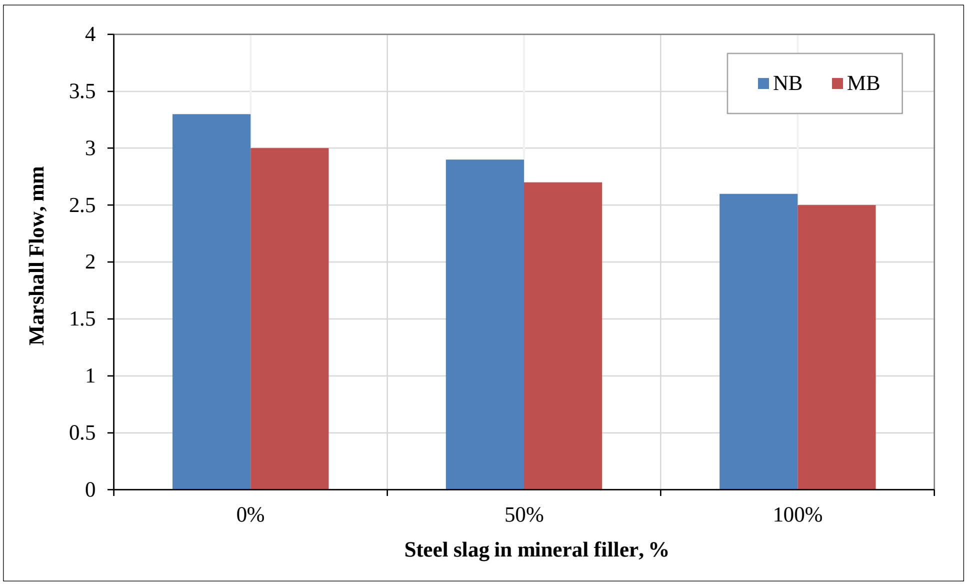

Figure 7. Marshall Flow of mixtures

Marshall Stiffness Index (MSI) is the ratio of Marshall stability in kN to the flow of the sample in mm. The higher the MSI, the stiffer the mixture and the better the resistance to shear and permanent deformation of asphalt concrete mixtures [41]. Figure 8 compares the MSI of the studied mixtures. It can be seen that both the SBS and SS help enhance the MSI. The combined use of both gives a further progressive improvement on the MSI when the SS filler content increases because steel slag has a larger angle of internal friction, angularity, and bulk specific gravity than limestone dust. The combined use of SS powder to replace all the LS dust filler and the SBS-modified binder generated the highest MSI value. This finding is also compatible with the similar work before, which used SS and copper mine tailings for mineral filler [19].

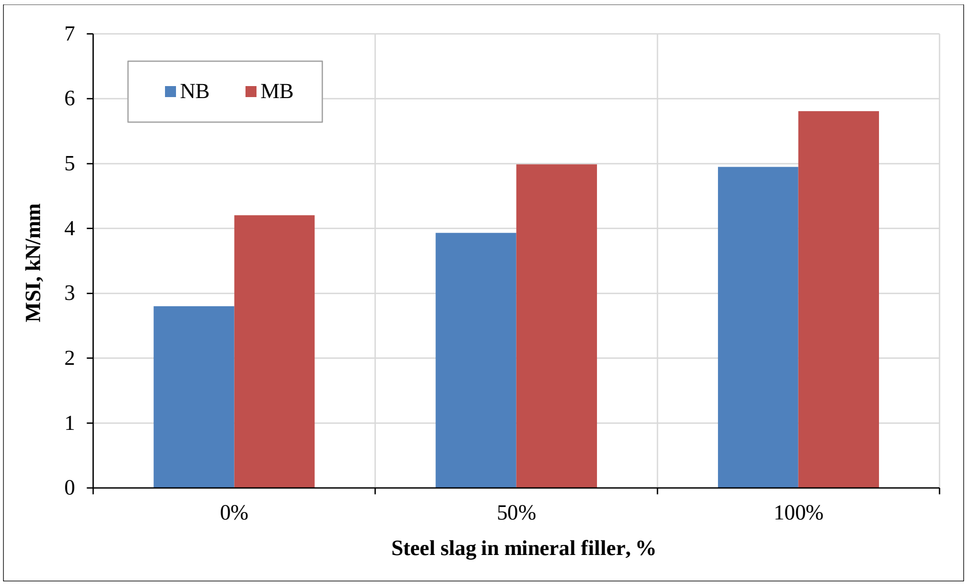

Figure 8. Marshall Stiffness Index (MSI) of Mixtures

3.2. The Indirect Tensile Test

Figure 9 presents the ITS results. Similar to the observations made during the Marshall tests, both the SBS binder modifier and the SS filler, when used individually, improved the ITS of the mixtures in both conditioned and unconditioned states. The combined use of both materials resulted in even greater enhancement. The mixture incorporating 100% SS along with the SBS-modified binder achieved the highest ITS. Fundamentally, SS possesses an alkaline nature, with a pH value of approximately 11.42, and exhibits pozzolanic properties due to its high chemical content of silica oxide and aluminum oxide. This composition promotes a pozzolanic reaction under alkaline conditions, generating a dense calcium-silicate-hydrate (C-S-H) gel, which enhances the bond with the asphalt binder [19, 42].

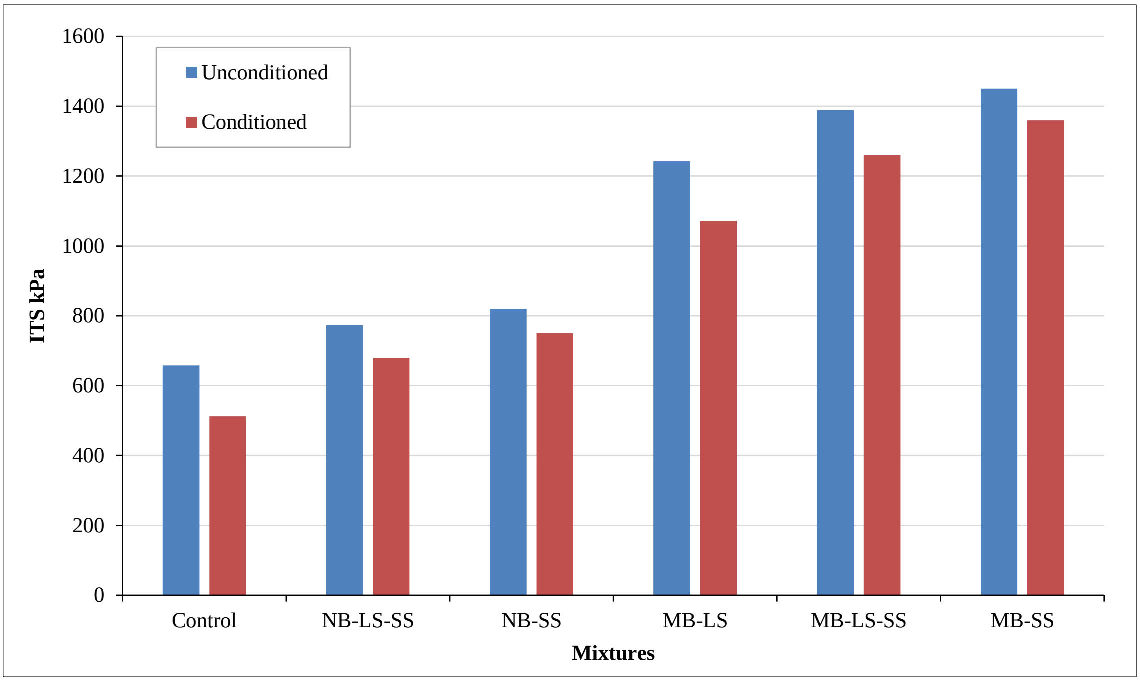

Figure 9. Indirect Tensile Strength (ITS) test results

Figure 10 compares the remaining tensile strength (RTS) of mixtures after conditioned freeze-thaw moisture exposure. RTS is the ratio of the ITS of a conditioned specimen to the ITS of an unconditioned specimen as expressed in Equation 1 below.

$$RTS = \frac{ITS\ conditioned}{ITS\ unconditioned} \tag{1}$$

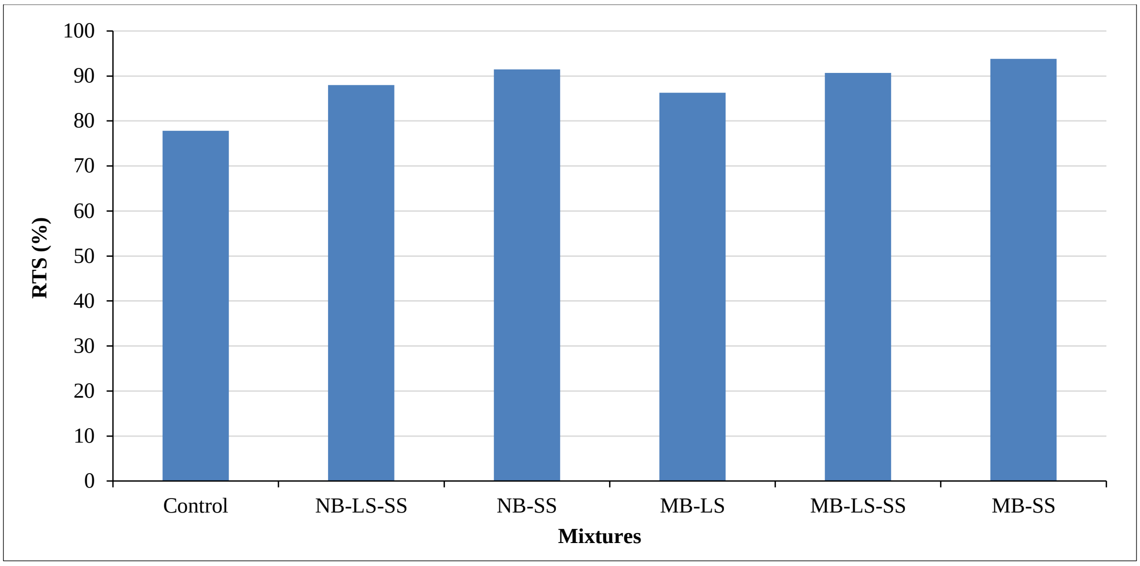

Figure 10. The Remaining Tensile Ratio results for the different types of mixtures

The higher the RTS value, the less the moisture susceptibility and the higher the resistance to stripping. It can be seen that either using SBS-modified binder or using SS for mineral filler alone can increase the RTS. However, the SS filler has a more pronounced effect on the mixture durability than the SBS asphalt binder. The result highlights the role of the chemical composition of SS in the adhesive strength to binder and the durability on moisture resistance of the mixtures [42]. The combined use of SBS asphalt binder and the SS filler together generated the best result, a result in agreement with the other similar work [19].

3.3. Scanning Electron Microscopy

Figure 11 compares SEM analysis of the SS particles and LS particles at three magnification scales. At the 5µm and 50 µm scales, it can be noticed that the crystal structure of SS particles presents an irregular 2D plate-form shape with sharp corners and a rough surface. The crystal structure of LS particles presents a regular shape of comparable 3D dimensions. In addition, the average crystal size of SS is bigger than that of LS. The SEM images at 500 µm scale show that SS particles displace a denser morphological texture of a high content of microscopic pores in comparison with the LS particles. Such a characteristic might be attributed to the plate shape of the SS crystal structure, which gives the SS particles themselves a high porosity and specific surface area. It also explains the capacity of SS to promote the adhesion of asphalt binders.

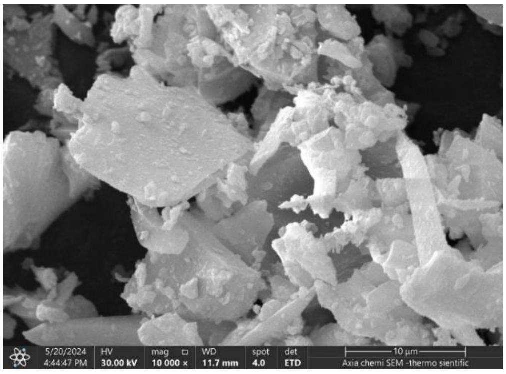

Steel slag particle at 10 µm scale

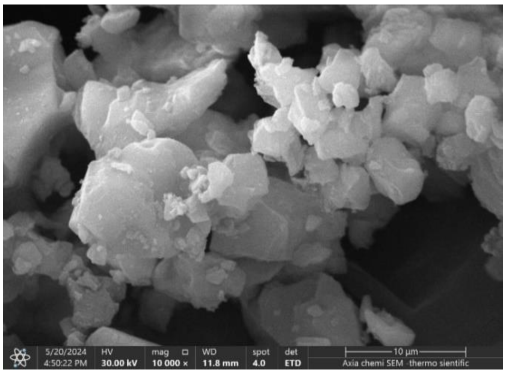

Limestone particle at 10 µm scale

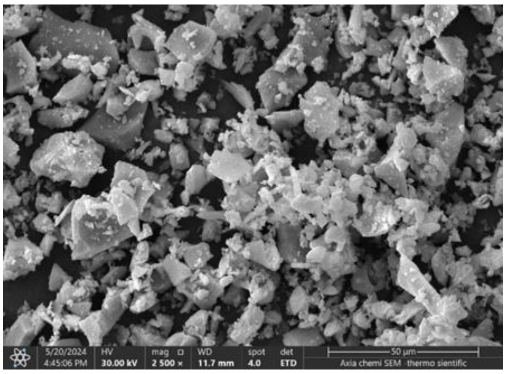

Steel slag particle at 50 µm scale

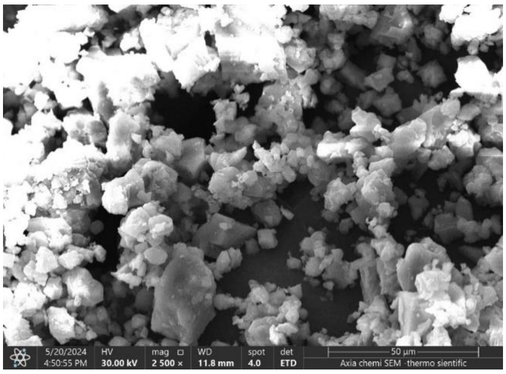

Limestone particle at 50 µm scale

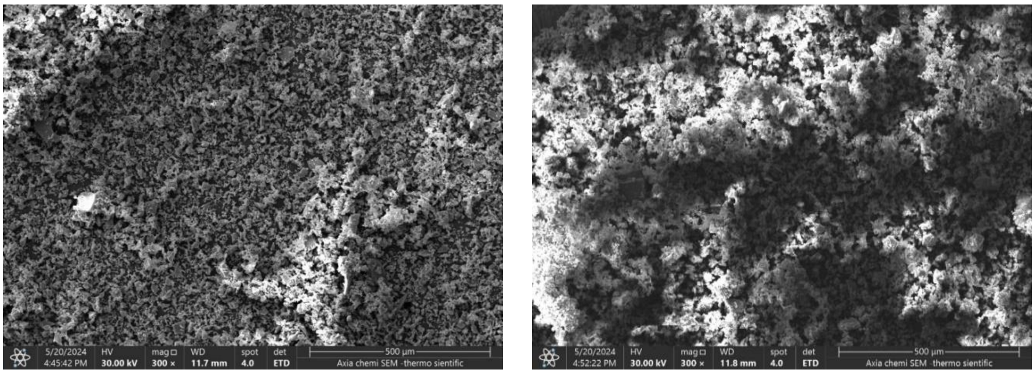

Steel slag particle at 500 µm scale Limestone particle at 500 µm scale

Figure 11. SEM images for the microscopic characteristics of SS and LS particles

Figure 12 shows the EDX results for the chemical composition of the two mineral fillers. Table 7 gives out the chemical composition examination, which shows that SS has a lower calcium content than LS. Although a high calcium oxide content is good for pavement because it reacts with water to generate calcium hydroxide (hydrated lime), a composition will enhance the resistance to rutting and fatigue cracking when present in asphalt mixtures. SS presents a high composition of carbon, silica oxide, and aluminum oxide. These components themselves can help increase the hardness of asphalt mixtures [42]. Most importantly, the silica oxide and aluminum oxide possess the pozzolanic nature, which promotes the pozzolanic reaction given the alkaline nature of SS itself. In addition, the presence of metallic components also helps enhance polishing resistance as well [42].

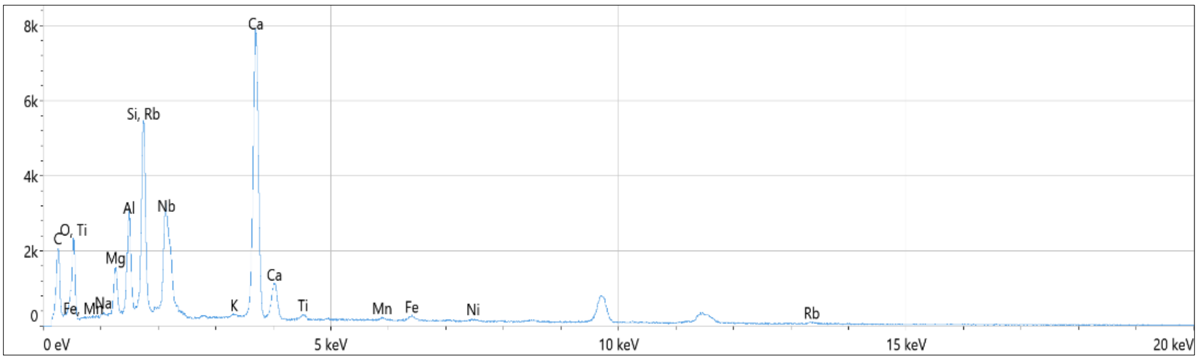

Steel Slag Particles

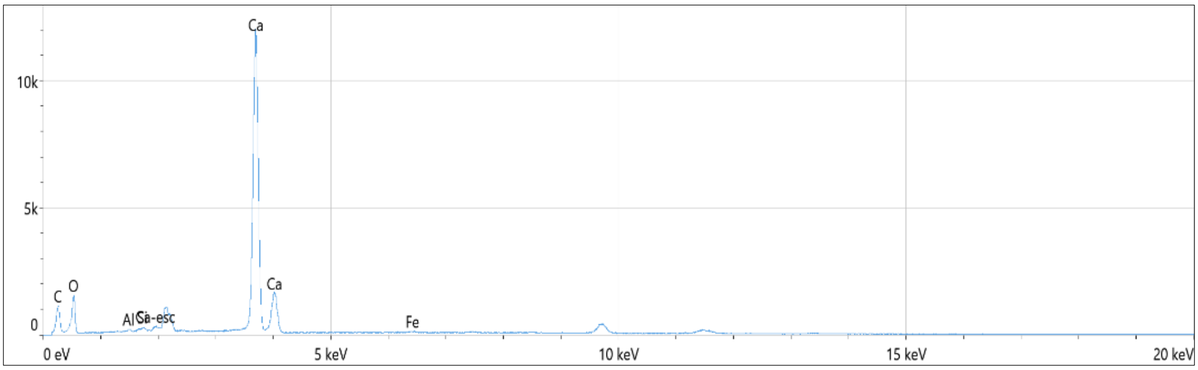

Limestone Particles

Figure 12. The EDX analysis results

Table 7. The chemical composition of limestone and steel slag

Constituent	Steel slag (%)	Limestone dust (%)
C	25.5	11.1
O	32.5	44.0
Mg	3.3	0.0
Al	5.3	0.2
Si	10.4	0.4
Ca	18.7	43.9
Fe	0.5	0.4

4. Conclusion

Asphalt concrete mixtures consume large quantities of natural resources, which has motivated researchers to explore the use of sustainable materials. This study aimed to evaluate the utilization of steel slag as a substitute for conventional limestone mineral filler, as well as the combined use of an SBS-modified binder to enhance the strength of asphalt mixtures. The designed mixtures included varying percentages of steel slag replacement: 0%, 50%, and 100%. The evaluation approach was based on two strategies: mechanical performance testing and microstructural analysis using SEM and EDX techniques. Mechanical performance was assessed through Marshall stability and flow tests, moisture susceptibility tests, and evaluation of volumetric properties. The results demonstrated that both the use of SBS-modified asphalt binder and the replacement of limestone filler with steel slag independently enhanced the Marshall stability and moisture resistance of asphalt mixtures. Moreover, the combined use of both materials provided even greater improvements, with the mixture incorporating 100% steel slag replacement exhibiting the best performance.

Steel slag particles possess higher porosity and specific surface area compared to limestone dust particles, attributed to the crystal structure of steel slag, which typically exhibits an angular, plate-like shape. This crystalline structure promotes better mechanical interlock among particles, resulting in increased mixture rigidity. Furthermore, the high porosity, larger surface area, and rough texture of the steel slag particles enhance binder-filler contact and improve adhesive bonding. EDX analysis confirmed the pozzolanic nature of the steel slag composition. The pozzolanic reaction further contributes to the enhancement of the mechanical properties of the asphalt mixtures.

5. Declarations

5.1. Author Contributions

Conceptualization, H.A. and A.A.; methodology, H.A.; software, A.A.; validation, Z.A. and Y.W.; formal analysis, A.A.; investigation, Y.W. and A.M.; resources, Z.A. and Y.W.; data curation, H.A. and A.A.; writing—original draft preparation, A.A. and Z.A.; writing—review and editing, H.A.; visualization, A.A. and A.M.; supervision, H.A. and A.A.; project administration, H.A.; funding acquisition, A.A., Z.A., H.A., and A.M. All authors have read and agreed to the published version of the manuscript.

5.2. Data Availability Statement

The data presented in this study are available in the article.

5.3. Funding

The authors received no financial support for the research, authorship, and/or publication of this article.

5.4. Conflicts of Interest

The authors declare no conflict of interest.

6. References

[1] Wang, Y., Latief, R. H., Al- mosawe, H., Mohammad, H. K., Albayati, A., & Haynes, J. (2021). Influence of iron filing waste on the performance of warm mix asphalt. Sustainability (Switzerland), 13(24), 13828. doi:10.3390/su132413828.

[2] Wei, Q., Ashaibi, A. Al, Wang, Y., Albayati, A., & Haynes, J. (2022). Experimental study of temperature effect on the mechanical tensile fatigue of hydrated lime modified asphalt concrete and case application for the analysis of climatic effect on constructed pavement. Case Studies in Construction Materials, 17. doi:10.1016/j.cscm.2022.e01622.

[3] Ashaibi, A. Al, Wang, Y., Albayati, A., Weekes, L., & Haynes, J. (2024). Uni- and tri-axial tests and property characterization for thermomechanical effect on hydrated lime modified asphalt concrete. Construction and Building Materials, 418. doi:10.1016/j.conbuildmat.2024.135307.

[4] Shi, K., Ma, F., Liu, J., Fu, Z., Song, R., Yuan, D., & Ogbon, A. W. (2024). Evolution of SBS-modified asphalt performance under aging and rejuvenation cycle conditions. Construction and Building Materials, 416. doi:10.1016/j.conbuildmat.2024.135156.

[5] Tian, Y., Li, H., Sun, L., Zhang, H., Harvey, J., Yang, J., Yang, B., & Zuo, X. (2021). Laboratory investigation on rheological, chemical and morphological evolution of high content polymer modified bitumen under long-term thermal oxidative aging. Construction and Building Materials, 303. doi:10.1016/j.conbuildmat.2021.124565.

[6] Mahmood, A. O., & Kattan, R. A. (2023). Improvement of Engineering Properties of Asphalt Binder and Mixture by Using SBS Additive Material. Advances in Civil Engineering, 7151175. doi:10.1155/2023/7151175.

[7] Li, N., Zhan, H., Yu, X., Tang, W., Yu, H., & Dong, F. (2021). Research on the high temperature performance of asphalt pavement based on field cores with different rutting development levels. Materials and Structures/Materiaux et Constructions, 54(2), 1-12. doi:10.1617/s11527-021-01672-3.

[8] Cui, Y., Cui, S., & Guo, L. (2022). Performance and Mechanism of Waste Oil Recycled SBS Modified Asphalt. Jianzhu Cailiao Xuebao/Journal of Building Materials, 25(2), 164–170. doi:10.3969/j.issn.1007-9629.2022.02.008.

[9] Li, H., Wang, H., Lin, J., Yang, J., & Yao, Y. (2024). Study on the Effect of SBS/HVA/CRM Composite-Modified Asphalt on the Performance of Recycled Asphalt Mixtures. Polymers, 16(22), 3226. doi:10.3390/polym16223226.

[10] Abed, M. A., Al-Tameemi, A. F., Abed, A. H., & Wang, Y. (2022). Direct tensile test evaluation and characterization for mechanical and rheological properties of polymer modified hot mix asphalt concrete. Polymer Composites, 43(9), 6381–6388. doi:10.1002/pc.26949.

[11] Pasetto, M., Baliello, A., Giacomello, G., & Pasquini, E. (2023). The Use of Steel Slags in Asphalt Pavements: A State-of-the-Art Review. Sustainability (Switzerland), 15(11), 8817. doi:10.3390/su15118817.

[12] Liu, J., & Guo, R. (2018). Applications of Steel Slag Powder and Steel Slag Aggregate in Ultra-High Performance Concrete. Advances in Civil Engineering, 1426037. doi:10.1155/2018/1426037.

[13] Song, Q., Guo, M.-Z., Wang, L., & Ling, T.-C. (2021). Use of steel slag as sustainable construction materials: A review of accelerated carbonation treatment. Resources, Conservation and Recycling, 173, 105740. doi:10.1016/j.resconrec.2021.105740.

[14] Yildirim, I. Z., & Prezzi, M. (2022). Subgrade stabilisation mixtures with EAF steel slag: an experimental study followed by field implementation. International Journal of Pavement Engineering, 23(6), 1754–1767. doi:10.1080/10298436.2020.1823389.

[15] Okan Sirin, R. T., & Sadek, H. (2014). Recycling of Local Qatar's Steel Slag and Gravel Deposits in Road Construction. International Journal of Waste Resources, 4(4), 1000167. doi:10.4172/2252-5211.1000167.

[16] Akbarnejad, S., Copuroglu, O., Houben, L. J. M., & Molenaar, A. A. A. (2012). Characterization of blast furnace slag to be used as road base material. Proceedings of the 7th International Conference on Maintenance and Rehabilitation of Pavements and Technological Control, 28-30 August, 2012, Auckland, New Zealand.

[17] Aziz, M. M. A., Shokri, M., Ahsan, A., Liu, H. Y., Tay, L., & Muslim, N. H. (2020). An Overview on Performance of Steel Slag in Highway Industry. Journal of Advanced Research in Materials Science, 67(1), 1–10. doi:10.37934/arms.67.1.110.

[18] Hosseinzadeh, N., Rezaei, M. J., & Hosseini, S. M. (2016). Investigation and performance improvement of hot mix asphalt concrete containing EAF slag. International Journal of Engineering and Technology, 8(4), 260–264. doi:10.7763/IJET.2016.V8.895.

[19] Oluwasola, E. A., Hainin, M. R., & Aziz, M. M. A. (2015). Evaluation of asphalt mixtures incorporating electric arc furnace steel slag and copper mine tailings for road construction. Transportation Geotechnics, 2, 47–55. doi:10.1016/j.trgeo.2014.09.004.

[20] Hassan, H. F., Al-Shamsi, K., & Al-Jabri, K. (2024). Effect of steel slag on the permanent deformation and life cycle cost of asphalt concrete pavements. International Journal of Pavement Research and Technology, 17(6), 1513-1530. doi:10.1007/s42947-023-00314-x.

[21] Ameri, M., Hesami, S., & Goli, H. (2013). Laboratory evaluation of warm mix asphalt mixtures containing electric arc furnace (EAF) steel slag. Construction and Building Materials, 49, 611–617. doi:10.1016/j.conbuildmat.2013.08.034.

[22] Zhao, X., & Zhang, Y. (2024). Analyzing the Mechanical and Durability Characteristics of Steel Slag-Infused Asphalt Concrete in Roadway Construction. Buildings, 14(3), 679. doi:10.3390/buildings14030679.

[23] Liu, J., Yu, B., & Hong, Q. (2020). Molecular dynamics simulation of distribution and adhesion of asphalt components on steel slag. Construction and Building Materials, 255. doi:10.1016/j.conbuildmat.2020.119332.

[24] Liu, J., Yu, B., Wang, S., Li, L., & Zhang, J. (2021). Use of tricalcium silicate to evaluate asphalt absorption on steel slag: Atomic simulation and micro-scale characterization. Measurement, 177, 109224. doi:10.1016/j.measurement.2021.109224.

[25] Wu, S., Xue, Y., Ye, Q., & Chen, Y. (2007). Utilization of steel slag as aggregates for stone mastic asphalt (SMA) mixtures. Building and Environment, 42(7), 2580–2585. doi:10.1016/j.buildenv.2006.06.008.

[26] Gao, J., Sha, A., Wang, Z., Tong, Z., & Liu, Z. (2017). Utilization of steel slag as aggregate in asphalt mixtures for microwave deicing. Journal of Cleaner Production, 152, 429–442. doi:10.1016/j.jclepro.2017.03.113.

[27] Li, S., Xiong, R., Zhai, J., Zhang, K., Jiang, W., Yang, F., Yang, X., & Zhao, H. (2020). Research Progress on Skid Resistance of Basic Oxygen Furnace (BOF) Slag Asphalt Mixtures. Materials, 13(9), 2169. doi:10.3390/ma13092169.

[28] Xu, H., Wu, S., Li, H., Zhao, Y., & Lv, Y. (2020). Study on recycling of steel slags used as coarse and fine aggregates in induction healing asphalt concretes. Materials, 13(4), 889. doi:10.3390/ma13040889.

[29] Bhupathi, S., Adepu, R., MVSS, S., Vijayapuri, V. R., & NR, D. M. (2025). Experimental evaluation of eco-friendly asphalt mixtures with recycled fine aggregates and steel slag. Innovative Infrastructure Solutions, 10(1), 1-21. doi:10.1007/s41062-024-01834-6.

[30] Gan, Y., Li, C., Zou, J., Wang, W., & Yu, T. (2022). Evaluation of the impact factors on the leaching risk of steel slag and its asphalt mixture. Case Studies in Construction Materials, 16. doi:10.1016/j.cscm.2022.e01067.

[31] Euroslag. (2025). Properties. The European Association Representing Metallurgical Slag Producers and Processors (Euroslag), Duisburg, Germany. Available online: https://www.euroslag.com/products/properties/ (accessed on March 2025).

[32] Zeinoddin, H. S., Abtahi, S. M., Hejazi, S. M., Babamohammadi, S., Goli, A., & Amuchi, M. (2016). Design and Production of Steel Slag Warm Mix Asphalt (SSWMA) Using an Amino-Based Resin. Transportation Infrastructure Geotechnology, 3(3–4), 91–108. doi:10.1007/s40515-016-0032-4.

[33] Abbas, A. S. (2020). Effect of fly ash and styrene butadiene rubber on the properties of hot mix asphalt. AIP Conference Proceedings, 2213. doi:10.1063/5.0000222.

[34] Abbas, H. F., & Abed, A. H. (2023). Enhancement of Hot Mix Asphalt stability by utilizing Cement Kiln Dust and Styrene-Butadiene-Styrene Polymer. Al-Nahrain Journal for Engineering Sciences, 26(2), 124-130. doi:10.29194/njes.26020124.

[35] Nie, Y., Liu, Q., Xiang, Z., Zhong, S., & Huang, X. (2023). Performance and Modification Mechanism of Recycled Glass Fiber of Wind Turbine Blades and SBS Composite-Modified Asphalt. Applied Sciences (Switzerland), 13(10), 6335. doi:10.3390/app13106335.

[36] Shen, A., Zhai, C., Guo, Y., & Yang, X. (2018). Mechanism of adhesion property between steel slag aggregate and rubber asphalt. Journal of Adhesion Science and Technology, 32(24), 2727–2740. doi:10.1080/01694243.2018.1507505.

[37] ASTM C127-15. (2024). Standard Test Method for Relative Density (Specific Gravity) and Absorption of Coarse Aggregate. ASTM International, Pennsylvania, United States. doi:10.1520/C0127-15.

[38] ASTM C131/C131M-20. (2020). Standard Test Method for Resistance to Degradation of Small-Size Coarse Aggregate by Abrasion and Impact in the Los Angeles Machine. ASTM International, Pennsylvania, United States. doi:10.1520/C0131_C0131M-20.

[39] ASTM C88/C88M-18. (2004). Standard Test Method for Soundness of Aggregates by Use of Sodium Sulfate or Magnesium Sulfate. ASTM International, Pennsylvania, United States. doi:10.1520/C0088_C0088M-18.

[40] Asphalt Institute Manual Series No. 02. (2015). MS-2 Asphalt Mix Design Methods. 7th Edition, Asphalt Institute, Lexington, United States.

[41] Zhang, J., Cooley, L. A., Hurley, G., & Parker, F. (2004). Effect of superpave defined restricted zone on hot-mix asphalt performance. Transportation Research Record, 1891, 103–111. doi:10.3141/1891-13.

[42] Hu, B., Huang, W., Yu, J., Xiao, Z., & Wu, K. (2021). Study on the adhesion performance of asphalt-calcium silicate hydrate gel interface in semi-flexible pavement materials based on molecular dynamics. Materials, 14(16), 4406. doi:10.3390/ma14164406.